The Scaffold Proteins Paxillin B and α-Actinin Regulate Septation in *Aspergillus nidulans* via Control of Actin Ring Contraction

Xiaogang Zhou,* Likun Zheng,* Luyu Guan,* Jing Ye,* Aleksandra Virag,† Steven D. Harris,‡,1 and Ling Lu*,1

*Jiangsu Key Laboratory for Microbes and Functional Genomics, College of Life Sciences, Nanjing Normal University, 210023, China, †DuPont Industrial Biosciences, 94304, and ‡Department of Biological Sciences, University of Manitoba, Winnipeg, Canada

ORCID IDs: 0000-0002-3365-652X (X.Z.); 0000-0001-5196-1977 (S.D.H.); 0000-0002-2891-7326 (L.L.)

ABSTRACT Cytokinesis, as the final step of cell division, plays an important role in fungal growth and proliferation. In the filamentous fungus *Aspergillus nidulans*, defective cytokinesis is able to induce abnormal multinuclear or nonnucleated cells and then result in reduced hyphal growth and abolished sporulation. Previous studies have reported that a conserved contractile actin ring (CAR) protein complex and the septation initiation network (SIN) signaling kinase cascade are required for cytokinesis and septation; however, little is known about the role(s) of scaffold proteins involved in these two important cellular processes. In this study, we show that a septum-localized scaffold protein paxillin B (PaxB) is essential for cytokinesis/septation in *A. nidulans*. The septation defects observed in a *paxB* deletion strain resemble those caused by the absence of another identified scaffold protein, α-actinin (AcnA). Deletion of α-actinin (AcnA) leads to undetectable PaxB at the septation site, whereas deletion of *paxB* does not affect the localization of α-actinin at septa. However, deletion of either α-actinin (*acnA*) or *paxB* causes the actin ring to disappear at septation sites during cytokinesis. Notably, overexpression of α-actinin *acnA* partially rescues the septum defects of the *paxB* mutant but not vice versa, suggesting AcnA may play a dominant role over that of PaxB for cytokinesis and septation. In addition, PaxB and α-actinin affect the septal dynamic localization of MobA, a conserved component of the SIN pathway, suggesting they may affect the SIN protein complex function at septa. Protein pull-down assays combined with liquid chromatography–mass spectrometry identification indicate that α-actinin AcnA and PaxB likely do not directly interact, but presumably belong to an actin cytoskeleton protein network that is required for the assembly and contraction of the CAR. Taken together, findings in this study provide novel insights into the roles of conserved scaffold proteins during fungal septation in *A. nidulans*.

KEYWORDS Paxillins; actinin; cytokinesis; septation; *Aspergillus nidulans*

CYTOKINESIS is a final step of cell division, by which a mother cell separates into two daughter cells (Green *et al.* 2012; D'Avino *et al.* 2015). Thus, cytokinesis is essential for survival to produce progenies by increasing the number of cells. In both animal cells and fungi, but not in higher plants, the contractile actin ring (CAR) functions as a dynamic tension-generating cellular machine that is essential for the cleavage of the mother cell to complete cytokinesis (von Dassow 2009; Laporte *et al.* 2010). However, cytokinesis is very complicated, and it is a highly regulated process that requires hundreds of proteins involved in CAR assembly, constriction, and disassembly (Laporte *et al.* 2010; Pollard and Wu 2010). In fungi, cytokinesis is always linked to septation, which requires the synthesis and delivery of special cell wall materials and formation of a structure known as the division septum (Cortés *et al.* 2007; Muñoz *et al.* 2013; Cortés *et al.* 2015). Normally, cytokinesis in fungi can be viewed as a four-stage process (Cheffings *et al.* 2016). First, landmark

doi: https://doi.org/10.1534/genetics.120.303234
Manuscript received January 15, 2020; accepted for publication April 12, 2020; published Early Online April 21, 2020.
Available freely online through the author-supported open access option.
Supplemental material available at figshare: https://doi.org/10.25386/genetics.12161718.
[1]Corresponding authors: Department of Biological Sciences, University of Manitoba, 212 Biological Sciences Bldg., Winnipeg, MB R3T 2N2, Canada. E-mail: Steven.harris@umanitoba.ca; and Jiangsu Key Laboratory for Microbes and Functional Genomics, College of Life Sciences, Nanjing Normal University, No.1 Wen Yuan Rd., Qi Xia Qu, Nanjing, China. E-mail: linglu@njnu.edu.cn

proteins accumulate at the division site of the cell to establish an appropriate site to ensure proper division (Bi and Park 2012; Akamatsu *et al.* 2014). Second, relevant scaffold proteins, which provide functions such as binding and supporting protein interactions, are transported to the division site to assist with the assembly of the actin ring (Ge and Balasubramanian 2008; Li *et al.* 2016). Third, a CAR composed of actin, septin, and formin is formed (Courtemanche 2018; Mela and Momany 2019). This step is regulated by a conserved signaling kinase cascade, such as the septation initiation network (SIN) in *Saccharomyces pombe* and the mitotic exit network in the budding yeast *S. cerevisiae* (Mulvihill *et al.* 2001; Corbett *et al.* 2006). The last step is accompanied by invagination of the plasma membrane for which the actin ring must be disassembled to ensure the complete abscission of the daughter cells to produce two individual cells.

Many lines of evidence have established that abnormal cytokinesis or septation can result in multinuclear or non-nucleated cells, which can block conidiation and lead to the formation of fluffy colonies in the filamentous fungus *Aspergillus nidulans* (McGuire *et al.* 2000; Bruno *et al.* 2001; Kim *et al.* 2006; Vargas-Muñiz *et al.* 2015). When the CAR is functional during cytokinesis, its protein complex must interact with numerous relevant scaffold proteins to anchor it to the plasma membrane or to transmit septation signals (Watanabe *et al.* 2008; D'Avino 2009; Zheng *et al.* 2018). Among these actin-relevant scaffold proteins, α-actinin, which was first isolated from rabbit skeletal muscle, is one of the best characterized members (Wu *et al.* 2001). Reducing α-actinin expression in animal cells results in muscle weakness and paralysis since it participates in myofibrillar organization (Shao *et al.* 2010). In addition, the localization of α-actinin to the cleavage furrow in mammalian cells also suggests that it is functional in cytokinesis (Jockusch *et al.* 1991). In the fission yeast *S. pombe*, an α-actinin-like protein Ain1 also localizes to the actin-containing medial ring during cytokinesis (Laporte *et al.* 2012), and strains lacking Ain1 only show abnormal cytokinesis and septation under stressful culture conditions (Wu *et al.* 2001). In the filamentous fungus *A. nidulans*, the Ain1 homolog α-actinin robustly accumulates at both of hyphal tips and septation sites, and loss of α-actinin completely abolishes the formation of the CAR and septation, indicating that α-actinin is essential for the organization of actin filaments (Wang *et al.* 2009). Another putative actin-binding scaffold protein, paxillin, has also been reported. Paxillin was initially characterized as a 68-kDa focal adhesion protein in tissues (Turner *et al.* 1991). In mammalian cells, paxillins play important roles in linking the extracellular matrix to the actin cytoskeleton and are required for cell migration and polarized cell growth (Brown and Turner 2004; Ge and Balasubramanian 2008). In *S. cerevisiae*, Pxl1p, a paxillin-like protein, participates in polarized cell growth (Mackin *et al.* 2004), while in *S. pombe*, the Pxl1p homolog Pxl1 is a conserved LIM domain-containing protein that modulates Rho1 activity and participates in cytokinesis (Pinar *et al.* 2008). Pxl1 localized to the medial ring requires its N-terminal region, whereas the LIM domain is necessary for its function. In addition, Pxl1-deleted cells form two rings, of which only one undergoes constriction and the rate of actin ring constriction is slower in Pxl1 deletion cells than that of wild type (Ge and Balasubramanian 2008). By contrast, little is known about the paxillin homologs in *A. nidulans*, in which the scaffold protein actinin is essential for cytokinesis and septation during CAR function.

In this study, we showed that a putative paxillin homolog, paxillin B (PaxB), but not PaxA (the *A. nidulans* homolog of *S. pombe* Pxl1), is required for proper cytokinesis and septation, and it shows a very similar phenotype with that of α-actinin, AcnA. Deletion of *acnA* or *paxB* caused the disappearance of actin rings. Furthermore, deletion of α-actinin led to undetectable PaxB at the septation site. By comparison, in the absence of PaxB, α-actinin was able to localize at septa but showed an abnormal ring shape, implying that α-actinin and PaxB are required for each other's functions. Findings in this study revealed that α-actinin and PaxB have some sequential or overlapping functions, while they also have independent roles in *A. nidulans*.

Materials and Methods

Strains, media, and culture conditions

All *A. nidulans* strains used in this study are summarized in Table 1. In general, the *A. nidulans* strains were grown on rich media, *i.e.*, YG (yeast + glucose), YAG (yeast + agar + glucose) or YAG supplemented with 5 mM uridine and 10 mM uracil (yeast + agar + glucose + uridine + uracil)), containing 2% glucose, 0.5% yeast extract, and 1 ml/liter 1000× trace elements; minimal media, *i.e.*, PGR (pyridoxine + glycerol + riboflavin) or PGR supplemented with 5 mM uridine and 10 mM uracil, containing 50 ml/liter salt, 1% glycerol, 0.5 mg/liter pyridoxine, 2.5 mg/liter riboflavin, and 1 ml/liter 1000× trace elements; or PDR (pyridoxine + glucose + riboflavin) (the carbon source-glycerol in PGR was replaced by glucose) or PDR supplemented with 5 mM uridine and 10 mM uracil media (Gupta *et al.* 1976; Jiang *et al.* 2017). The growth conditions, crosses, DNA transformation procedures, and induction conditions for *alcA(p)*-driven expression were performed as previously described (Osmani *et al.* 1988; Liu *et al.* 2003; Todd *et al.* 2007).

Construct design and protein tagging

All primers used in this study are shown in Table 2. To generate the *paxB* (or *paxA*) deletion cassette, the fusion PCR method was used as previously described. Briefly, ∼1 kb of the upstream and downstream flanking sequences of the *paxB* (*paxA*) gene were amplified using primers paxB-P1/P3 (paxA-p1/p3) and paxB-P4/P6 (paxA-p4/p6), respectively, with genomic DNA (gDNA) of TN02A7 as a template. The primers pyroA-F/R were used to amplify the *pyroA*

Table 1 *A. nidulans* strains used in this study

Strain	Genotype	Source
R21	*pabaA1*; *yA2*	FGSC
TN02A7	*pyrG89*; *pyroA4*, *nkuA::argB2*; *riboB2*, *veA1*	FGSC
GQ1	*pyrG89*; *sepH 1*; *chaA1*; *veA1*	Bruno *et al.* (2001)
WJ03	*pyrG89*; *ΔacnA::pyrG*; *pyroA4*, *nkuA::argB2*; *riboB2*, *veA1*	Wang *et al.* (2009)
AAV126	*pyrG89*; *argB2*; *pyroA4*, *ΔpaxA::pyroA*, *nkuA::argB*; *veA1*	This study
AAV127	*pyrG89*; *ΔpaxB::pyroA*; *argB2*; *pyroA4*, *nkuA::argB*; *veA1*	This study
AAV156	*pyrG89*; *argB2*; *pyroA4*, *ΔpaxA::pyr4*, *nkuA::argB*; *veA1*	This study
AAV157	*pyrG89*; *ΔpaxB::pyr4*; *argB2*; *pyroA4*, *nkuA::argB*; *veA1*	This study
WJ02	*pyrG89*; *alcA(p)::gfp-acnA::pyr4*, *pyroA4*, *nkuA::argB2*; *riboB2*, *veA1*	Wang *et al.* (2009)
AAV97	*pyrG89*; *alcA(p)::gfp-paxA::pyr4*, *pyroA4*, *nkuA::argB2*; *riboB2*, *veA1*	This study
AAV98	*pyrG89*; *alcA(p)::gfp-PaxB::pyr4*; *pyroA4*, *nkuA::argB2*; *riboB2*, *veA1*	This study
SNT147	*pyrG89*; *argB2*; *ΔnkuA::argB*; *pyroA4*; *alcA(p)::gfp-tpmA::pyr-4*	Bergs *et al.* (2016)
WR01	*pyrG89*, *alcA(p)::gfp-mobA::pyr4*; *pyroA4*, *nkuA::argB2*; *riboB2*, *veA1*	This study
ZXB01	*pyrG89*; *ΔacnA::pyroA*, *pyroA4*, *nkuA::argB2*; *riboB2*, *veA1*	This study
ZXB02	*pyrG89*, *alcA(p)::gfp-mobA::pyr4*; *ΔacnA::pyroA*, *pyroA4*, *nkuA::argB2*; *riboB2*, *veA1*	This study
ZXB03	*pyrG89*, *alcA(p)::gfp-mobA::pyr4*; *ΔpaxB::pyroA*; *pyroA4*, *nkuA::argB2*; *riboB2*, *veA1*	This study
ZXB04	*pyrG89*; *ΔpaxB::pyroA*; *argB2*; *pyroA4*, *ΔnkuA::argB*; *alcA(p)::gfp-tpmA::pyr-4*; *veA1*	This study
ZXB05	*pyrG89*; *argB2*; *ΔacnA::pyroA*, *ΔnkuA::argB*, *pyroA4*; *alcA(p)::gfp-tpmA::pyr-4*; *veA1*	This study
ZXB06	*pyrG89*; *alcA(p)::gfp-paxB::pyr4*; *ΔacnA::pyroA*, *pyroA4*, *nkuA::argB2*; *riboB2*, *veA1*	This study
ZXB07	*pyrG89*; *ΔpaxB::pyroA*; *alcA(p)::gfp-acnA::pyr4*, *pyroA4*, *nkuA::argB2*; *riboB2*, *veA1*	This study
ZXB08	*pyrG89*; *ΔpaxB::pyroA*; *gpd(p)::acnA-pyroA4*, *pyroA4*, *nkuA::argB2*; *riboB2*, *veA1*	This study
ZXB09	*pyrG89*; *gpd(p)::paxB -pyroA4*; *ΔacnA::pyroA*, *pyroA4*, *nkuA::argB2*; *riboB2*, *veA1*	This study
ZXB10	*pyrG89*; *gpd(p)::gfp -pyroA4*; *pyroA4,nkuA::argB2*; *riboB2*, *veA1*	This study
ZXB11	*pyrG89*; *alcA(p)::gfp-paxB::pyr4*; *sepH 1*; *chaA1*; *veA1*	This study
ZXB12	*pyrG89*; *sepH 1*; *alcA(p)::gfp-acnA::pyr4*; *chaA1*; *veA1*	This study
ZXB13	*pyrG89*; *argB2*; *pyroA4*, *ΔpyroA::paxB-pyrG*, *ΔnkuA::argB*; *veA1*	This study
ZXB14	*pyrG89*; *gpd(p)::paxB-flag*; *alcA(p)::gfp-acnA::pyr4*, *nkuA::argB2*; *riboB2*, *veA1*	This study
ZXB15	*pyrG89*; *pyroA4*, *nkuA::argB2*; *gpd(p)-flag-riboB2*; *veA1*	This study

fragment with the template gDNA of R21. Next, the three aforementioned PCR products were used as templates for amplification using the primer pair paxB-P2/P5 (paxA-p2/p5) to generate the cassette, which was then transformed into the recipient strain TN02A7.

To generate the *alcA(p)::*gfp-paxB strain, a 948-bp truncated genomic sequence of *paxB* (a full length of *paxB* is 2513 bp) was amplified by PCR from wild-type TN02A7 gDNA using the primers alc-paxB-F/R (the *paxB* start codon has been changed to CTG). The PCR product was digested with NotI and XbaI and then ligated into the pLB01 plasmid resulting in the addition of a GFP tag on the N terminus of *paxB*, and then the resulting plasmid was transformed into the recipient strain TN02A7. As shown in Supplemental Material, Figure S2A, a homologous integration of truncated genomic sequence of *paxB* yielded a full-length *paxB* fused to the GFP-coding sequence under the control of the *alcA* promoter accompanied with an extra truncated copy of *paxB*. A *paxA* fragment (824 bp) was amplified from TN02A7 gDNA using the primers alc-paxA-F/R. Then, a similar strategy was used to generate *alcA(p)::*gfp-paxA strain.

To generate the construct for the *paxB* overexpression strain, a *paxB* DNA fragment was amplified using the *gpd-paxB*-F/R as primers and gDNA of TN02A7 as a template. The PCR fragment was then cloned into the aforementioned *AngpdA* promoter-carrying vector pBARGPE1. The resulting plasmid was transformed into the recipient strain TN02A7.

To generate the *paxB* complementation strain, ~1 kb of the upstream and downstream flanking sequences of the *paxB* were amplified using primers c-paxB-P1/P3 and c-paxB-P4/P6, respectively, with gDNA of TN02A7 as a template. The primers pyrG-F/R were used to amplify the *pyrG* fragment with the template plasmid PXDRFP. Next, the three aforementioned PCR products were used as templates for amplification using the primer pair c-paxB-P2/P5 to generate the cassette, which was then transformed into the recipient strain, *paxB* deletion strain (AAV127).

RNA isolation and quantitative real-time PCR

To isolate RNA from the relevant strains, fresh conidia or hyphal cells were inoculated on minimal medium in the dark for 24 hr at 37°, and the mycelia were immediately harvested and frozen in liquid nitrogen. Total RNA was extracted using TRIzol (Roche) as directed by the manufacturer's instructions. For gDNA digestion and complementary DNA synthesis, the HiScript II Q RT SuperMix for qPCR (+gDNA wiper) Kit (Vazyme Biotech) was used, following the procedures in the protocol manual.

Microscopy and image processing

For the microscopic observations, conidia or hyphal cells were inoculated onto sterile glass coverslips at the relevant temperatures before observation. Hyphal septa were stained using calcofluor white (CFW; Sigma Aldrich, St. Louis,

Table 2 Primers used in this study

Primer name	DNA sequence 5′–3′
paxA-p1	CATGCGATTGAAGTGTCGAC
paxA-p2	GGAAGTGATGCGTGTGACTC
paxA-p3	CTTCTTCCTCTGTCGTGCTTTCG CTTGACGAACACGCGGTCTC
paxA-p4	GTCCTCAAGACCCACTACGAGACTTGCCCATGATCAAATG
paxA-p5	CCTCGCATATGCTGATGATAG
paxA-p6	GCATCGGCGAGCACTGGTCT
paxA-F	GATATACGGACGCAGTGAAC
paxA-R	CCCAGTTTCGTTCCGAGGGT
acnA-p1	CTTCTCCAGCGCTTGCCATAGC
acnA-p2	CGTAGAACTGCGCAGTGTCGAT
acnA-p3	CTATTATCTGACTTACCCGCCAAGTTGAGCGATATGCAGGTTC
acnA-p4	CCAAGAGAAAGCGTCAAGTCAGCGTGTGATCCGTTCTTAATC
acnA-p5	CTGTACGTAACGTAGGCGACG
acnA-p6	ATCCTCCATCTCCTGGTCGAG
acnA-F	AGAGGGTAGAAAATGCGGGA
acnA-R	ATACATGGCAAACTGGGAGG
paxB-p1	ATGTCTGGACTGGCAACACC
paxB-p2	GACGTGGCTGACAGTCAAAG
paxB-p3	CTTCTTCCTCTGTCGTGCTTTCG CTTGATGGGCAATCGATATC
paxB-p4	GTCCTCAAGACCCACTACGAGTGGCTTTGGTAGTAGGTG
paxB-p5	GTCTCTCCCACAATTGTCTC
paxB-p6	GTAGGAGGCTGAGATGCGAT
paxB-F	AATCTTCCCCCACGAGCTAC
paxB-R	GACGACTTCAGACGAATGCC
alc-paxA-F	AGCAGCGGCCGCTGGCATCAGACATGGGCGACT
alc-paxA-R	AACCTCTAGACACACGTCGTCGACATCGAG
alc-paxB-F	AGCAGCGGCCGCTGATCCACCGGTCCCCTCTTC
alc-paxB-R	AACCTCTAGACCTGGGAGAACTCTCCTCGC
gpd-acnA-F	GGGCCGCCACTCCACCGGCGCCTTGACGGTTGACGAGTCGTG
gpd-acnA-R	CTCGAGGTCGACGGTATCGATTCACACGCTGCCGTTGATAG
gpd-paxB-F	CCTTTAATCAAGCTTATCGATATGATCCACCGGTCCCCTCTTCA
gpd-paxB-F	CTCGAGGTCGACGGTATCGATTCAGGCCCTAGGAGACGACTT
RT-acnA-F	AGAGGGTAGAAAATGCGGGA
RT-acnA-R	ATACATGGCAAACTGGGAGG
RT-paxB-F	GGCATGTCGGTCACTTCTTCTGC
RT-paxB-R	CGCCTACAGCAGTGATCACG
c-paxB-p1	CACACTAGGTTCACAACGCAGG
c-paxB-p2	GGTCACCAGACTTTGCAGCTAC
c-paxB-p3	CTCTAGATGCATGCTCGAGCTCAGGCCCTAGGAGACGACTTC
c-paxB-p4	CAGTGCCTCCTCTCAGACAGTTGTGGCTTTGGTAGTAGGTG
c-paxB-p5	GGTTCAACTAACGTCTGGTTCAG
c-paxB-p6	CACCACGATTGAATCAGGGATG
PyrG-F	GCTCGAGCATGCATCTAGAG
PyrG-R	CTGTCTGAGAGGAGGCACTG

MO). Differential interference contrast and fluorescence images of the live cells were collected with a Zeiss Axio imager A1 microscope (Zeiss, Jena, Germany) and then processed with Adobe Photoshop (Adobe, San Jose, CA). The detailed procedure was described previously.

Protein extraction, α-actinin-GFP purification, and Western blot analysis

Fresh conidia were inoculated into minimal PGR medium and incubated for 24 hr at 37°, and then mycelia were harvested and immediately frozen in liquid nitrogen. For protein extraction, the following lysis buffer recipe was used: 10 mM Tris-HCl, pH 7.5, 150 mM NaCl, 0.5 mM EDTA, 0.01% Triton X-100, 1 mM DTT, 1 mM PMSF, and 1:100 protease inhibitor cocktail. Briefly, the fungal tissue was ground in liquid nitrogen (1.5∼2 mg wet weight, approximately) and then suspended in 5 ml of lysis buffer. The samples were then centrifuged at 5000 rpm for 10 min at 4°, and the supernatant was then transferred to another centrifuge tube. The crude supernatant was then clarified via centrifugation at 7000 rpm for 15 min at 4°. The protein supernatant was then gently mixed with the GFP-Trap resin (35 μl), followed by incubation at 4° for 2 hr. Next, the pelleted GFP-Trap resin was washed once in 500 μl of ice-cold dilution buffer (10 mM Tris-HCl, pH 7.5, 150 mM NaCl, 0.5 mM EDTA, 1 mM PMSF, 1:100 protease inhibitor cocktail) and twice with 500 μl of wash buffer (10 mM Tris-HCl, pH 7.5, 350 mM NaCl, 0.5 mM EDTA, 1 mM PMSF, 1:100 protease inhibitor cocktail). The

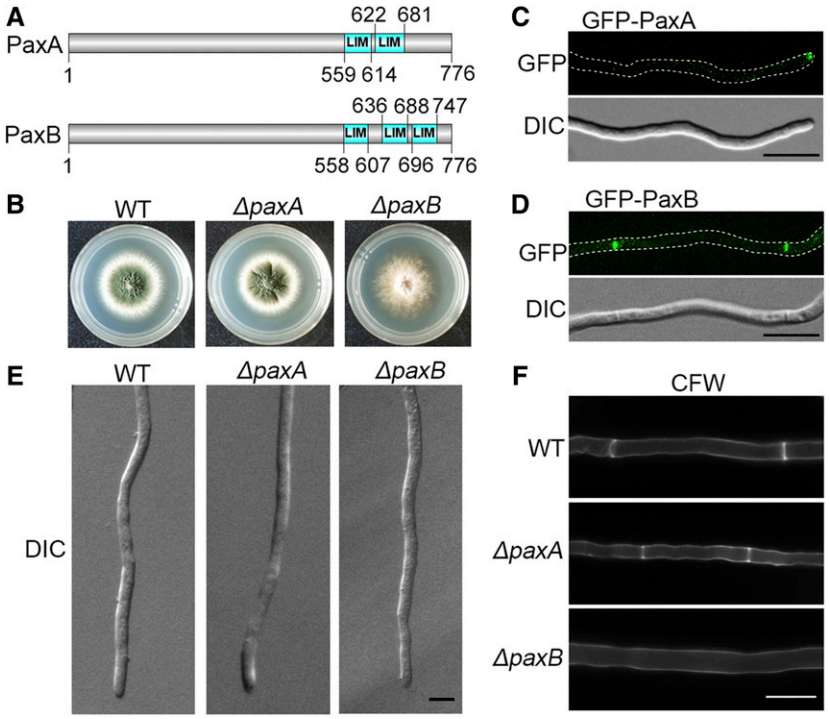

Figure 1 Identification and analysis of the paxillin proteins in *A. nidulans*. (A) Domain analysis of PaxA and PaxB via the SMART algorithm (http://smart.embl-heidelberg.de/). (B) Colony morphologies of the wild-type (TN02A7), *ΔpaxA* (AAV126), and *ΔpaxB* (AAV127) strains cultured on YAG medium supplemented with 5 mM uridine and 10 mM uracil (YUU) at 37° for 2 days. (C) Localization of GFP-PaxA and (D) GFP-PaxB expressed under the control of the *alcA* conditional promoter in AAV97 and AAV98 cells cultured in liquid PGR minimal media. Bar, 10 μm. (E) Differential interference contrast (DIC) images comparing the polar growth in the parental wild-type strain (TN02A7) and the *ΔpaxA* (AAV126) and *ΔpaxB* (AAV127) strains cultured in liquid YUU media at 37° for 16 hr. Bar, 10 μm. (F) Comparison of septum formation in the hyphal cells of the wild-type (TN02A7), *ΔpaxA* (AAV126), and *ΔpaxB* (AAV127) strains cultured on liquid YUU medium at 37° for 20 hr. Bar, 10 μm.

liquid chromatography–tandem mass spectrometry was performed at Wuhan GeneCreate Biological Engineering, as a commercial service. The Flag-Trap assay was carried out by a similar strategy to that of GFP-Trap. For Western blot analysis, protein samples were loaded onto a 10% SDS polyacrylamide gel and transferred to a PVDF membrane (Immobilon-P; Millipore, Bedford, MA) in transfer buffer (384 mM glycine, 50 mM Tris, pH 8.4, 20% methanol) at 350 mA for 1.5 hr. Next, the membrane was blocked with PBS, 5% milk, and 0.1% Tween 20 and then probed with anti-GFP mouse monoclonal antibody (catalog number 11 814 460 001; Roche).

Data availability

Strains and plasmids are available upon request. The authors affirm that all data necessary for confirming the conclusions of the article are present within the article, figures, and tables. Supplemental material available at figshare: https://doi.org/10.25386/genetics.12161718.

Results

Identification and analysis of paxillin proteins in A. nidulans

To identify putative fission yeast paxillin-related protein Pxl1 homologs in *A. nidulans*, a BLASTp search using the Pxl1 amino-acid sequence as a query was performed in the NCBI database. The searching yielded two putative paxillin proteins, which are now referred to as *paxA* (GenBank accession no. AN7626) and *paxB* (GenBank accession no. AN3659). *paxA* encodes a protein with a total length of 776 amino acids. A Simple Modular Architecture Research Tool (SMART) conserved domain analysis showed that *paxA* encodes a protein with two LIM domains, a typical conserved paxillin protein domain, and that *paxB* encodes a 776-amino acid protein with three LIM domains (Figure 1A). In addition, we found that PaxA and PaxB share 35 and 37% amino acid sequence identity with the *S. pombe* paxillin protein Pxl1, respectively. To further investigate functions of these paxillin proteins in *A. nidulans*, the *paxA* and *paxB* deletion strains (referred to as AAV126 and AAV127, as shown in Figure 1B and Figure S1C) and the conditional *alcA(p)::*gfp-paxA and *alcA(p)::*gfp-paxB strains (referred to as AAV97 and AAV98, as shown in Figure S2B) were constructed via homologous integration. All aforementioned deletion strains and GFP-labeling strains have been verified by diagnostic PCR, as shown in Figure S1, A and B and Figure S2A, indicating the strains were constructed as predicted. In addition, GFP labeling strains showed no detectable phenotypic differences compared to that of its parental wild-type strain either in colony size or in conidial production (Figure S2B), suggesting GFP labeling strains were fully functional. To further confirm the phenotype of relative deletion strains, *paxA* and *paxB* deletion strains (referred to as AAV156 and AAV157) were again constructed with another selection marker *pyr4*, as shown in Figure S1C, two types of independent *ΔpaxA* strains (AAV126 and AAV156) showed no detectable difference compared to the parental wild-type strain TN02A7. By comparison, both *ΔpaxB* strains (AAV127 and AAV157) exhibited consistent abolished conidiation phenotype. Subsequent fluorescence microscopy showed that GFP-PaxA highly accumulated at the tips of the hyphal cells, while GFP-PaxB was highly

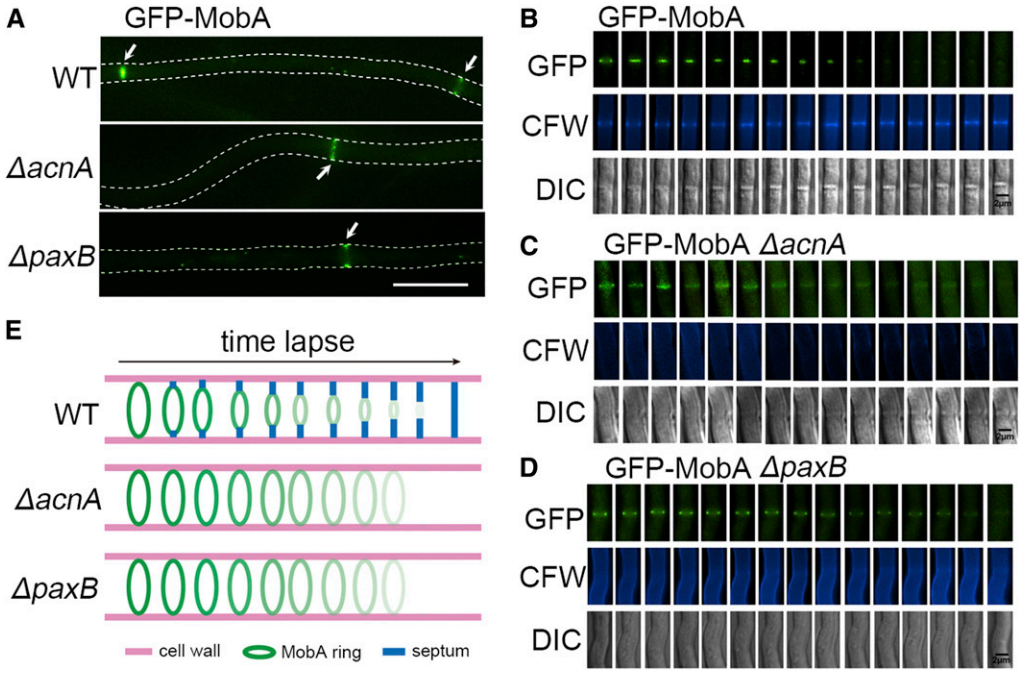

Figure 2 PaxB and α-actinin affected septal dynamic localization of MobA, a conserved component of the SIN pathway. (A) Localization of GFP-MobA in the wild-type (WR01), *ΔacnA* (ZXB02), and *ΔpaxB* (ZXB03) strains cultured in liquid minimal PGR medium at 37° for 20 hr. Bar, 10 μm. CFW-stained septa, localization of GFP-MobA, and differential interference contrast (DIC) images of the wild-type (WR01) (B), *ΔacnA* (ZXB02) (C), and *ΔpaxB* (ZXB03) (D) strains cultured in liquid minimal PGR medium at 37° for 20 hr. Bar, 2 μm. (E) A schematic model of septation and the dynamics of the GFP-MobA ring in the wild-type (WR01), *ΔacnA* (ZXB02), and *ΔpaxB* (ZXB03) strains.

localized at the septa (Figure 1, C and D), suggesting that PaxA and PaxB could have different functions such that PaxA might be required for polar growth of the hyphal cells and PaxB might play roles in cytokinesis. To verify the aforementioned hypothesis, hyphal cells of the *ΔpaxA* and *ΔpaxB* strains and their parental wild-type strain were examined via microscopy. The *ΔpaxA* and *ΔpaxB* strains showed no visible differences in their hyphal polarity compared with that of the wild-type strain (Figure 1E). In contrast, when these strains were visualized after staining with the chitin dye CFW, as shown in Figure 1F, septa were observed in the wild-type and *ΔpaxA* strains, while no CFW-stained septa were detected in the *ΔpaxB* strain, suggesting that PaxB is required for septum development in *A. nidulans*. Moreover, a *paxB* complementary strain (ZXB13) was constructed by transforming the *paxB* gene at the original loci to the *paxB* deletion background strain (AAV127). As shown in Figure S1D, colony comparisons showed that there was no detective difference between the *paxB*-complementation strain (ZXB13) and the wild-type control TN02A7, which suggested that phenotype of the *paxB* deletion strain was results from loss of PaxB.

The septum-abolished phenotype of deletion in *paxB* was very similar to that resulting from loss of the scaffold protein, α-actinin (AcnA), which has been previously been identified as an essential factor for cytokinesis (Wang *et al.* 2009). As shown in Figure S3, compared with the reference wild-type strain, the *ΔacnA* strain showed complete loss of conidiation and septum formation accompanied by reduced hyphal growth in the colony. Moreover, no cleistothecium could be found in the *ΔacnA* and *ΔpaxB* strains (Figure S3A), indicating that both the asexual and sexual processes were disrupted. These data suggest that cytoskeletal proteins α-actinin (AcnA) and PaxB are required for cytokinesis/septation and conidiation in *A. nidulans*.

PaxB and α-actinin affect septal dynamic localization of MobA, a conserved component of the SIN pathway

Previous studies have shown that a conserved SIN is required for cytokinesis/septation (Harris 2001). MobA/SidB, the last component in the core SIN protein kinase cascade, must translocate from the site of the spindle pole body to the septum site and then contract accordingly with the CAR (Kim *et al.* 2006). Considering PaxB and α-actinin are scaffold proteins, they might perform important functions by affecting the localization or stability of other members of a cytokinesis-related protein complex. Thus, we proposed that the defective phenotypes in the *ΔacnA* and *ΔpaxB* strains were most likely due to mislocalization of the SIN components. To further visualize changes in the localization of MobA in hyphal cells induced by deletion of α-actinin or *paxB*, a GFP moiety was added to the N terminus of MobA in the wild-type (R21), *ΔacnA*, and *ΔpaxB* backgrounds, generating strains referred as WR01, ZXB02, and ZXB03, respectively. As predicted, in the wild-type strain, GFP-MobA could form an actin ring-like structure during the initiation of septation (Figure 2A) that gradually contracted to form a dot in the middle center of the septum site. Finally, this dot disappeared once septum formation was completed as shown in the time-lapse images (Figure 2, B and E). Interestingly, in the *ΔacnA* and *ΔpaxB* strains, GFP-MobA could also form an actin ring-like structure (Figure 2A), but no further contraction was observed under the same observation and culture conditions. This observation suggests that both α-actinin and PaxB affect proper

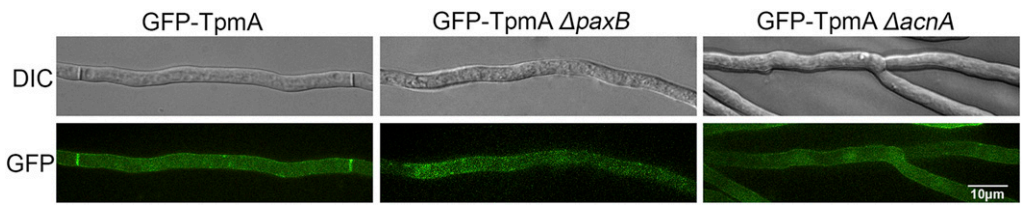

Figure 3 Deletion of *paxB* and *acnA* abolished actin ring formation. Localization of the actin filament-stabilizing protein GFP-TpmA in the wild-type (SNT147), *ΔpaxB* (ZXB04), and *ΔacnA* (ZXB05) strains cultured in liquid minimal PDR medium at 37° for 20 hr. Bar, 10 μm.

movement of MobA at septation sites during the CAR process (Figure 2, C–E).

To further clarify the relationship between the SIN protein kinase cascade and PaxB or α-actinin, we further examined the localization of PaxB or α-actinin in an SIN-defective background by using a strain carrying the temperature-sensitive *sepH 1* allele. SepH is a key protein kinase in the SIN (Bruno *et al.* 2001). Surprisingly, no GFP-α-actinin or GFP-PaxB signal was detected at the septation site in the *sepH 1* background at the restrictive temperature (42°) (Figure S4), suggesting that SepH is required for the localization of PaxB and α-actinin to septation sites.

The CAR, a dynamic apparatus, must invaginate with the cell membrane during the completion of cytokinesis (Yumura and Kitanishi-Yumura 1990). To further test whether the defective contraction of the GFP-MobA ring induced by PaxB or α-actinin deletion is linked to the function of the CAR, an actin filament-stabilizing protein, TpmA (Evangelista *et al.* 2002; Pearson *et al.* 2004; Bergs *et al.* 2016), was tagged with GFP at its N terminus in the wild-type (TN02A7), *ΔpaxB*, and *ΔacnA* background strains to generate strains referred to as SNT147, ZXB04, and ZXB05, respectively. As shown in Figure 3, fluorescence microscopy showed that GFP-TpmA showed a ring-like structure at septation sites during septum formation in the parental wild-type strain, consistent with the findings of previous studies. However, neither the GFP-TpmA ring structure nor septa were found in the *ΔpaxB* and *ΔacnA* strains (Figure 3), implying that α-actinin and PaxB are required for actin ring or CAR formation.

α-Actinin AcnA and PaxB depend on each other with different contents for localization and functions

Considering that α-actinin and *paxB* deletion strains showed similar septum-abolished phenotypes, we hypothesized that α-actinin and PaxB might depend on each other for their proper involvement in CAR formation during cytokinesis. Therefore, we next explored whether α-actinin and PaxB depend on each other for proper localization. As shown in Figure 4A, GFP-PaxB was localized at septation sites in a ring-like structure in the wild-type strain; however, no GFP-PaxB ring structure was found in the *ΔacnA* strain. In comparison, in the absence of *paxB*, the ring-like structure of GFP-α-actinin was still found, but it showed three different defective contractile patterns (Figure 4E, iii and iv). As shown in the time lapse fluorescence images in Figure 4B, two patterns of GFP-α-actinin ring structures, *i.e.*, no start (Figure 4Ei) and start (Figure 4Eii), were detected in the hyphal cells of the wild-type strain. These structures contracted to form a dot at the centers of the hyphal cells and then disappeared at the end of cytokinesis (Figure 4C). However, deletion of *paxB* caused GFP-α-actinin to form a curly band and then to accumulate as a dot at the putative septation sites in the hyphal cells (Figure 4D). These data suggest that α-actinin and PaxB affect each other to some contents for their localization and functions during cytokinesis/septation.

Overexpression of α-actinin partially rescues the defects of the paxB mutant, but not vice versa

The aforementioned data suggested that α-actinin and PaxB may have similar functions during the process of cytokinesis. Next, we further tested whether α-actinin and PaxB share complementary functions by introducing *paxB* or α-actinin overexpression constructs into the *ΔacnA* and *ΔpaxB* (ZXB08 and ZXB09) backgrounds, respectively. Real-time PCR verification indicated that the *paxB* and α-actinin *acnA* mRNA expression levels were upregulated by ∼27- and 43-fold in the ZXB08 and ZXB09 strains, respectively (Figure S5), indicating that the overexpression strains were successfully constructed. The OE-*paxB ΔacnA* (ZXB08) strain showed a small and fluffy colony phenotype (Figure 5A). Furthermore, the fluorescence microscopic image showed that no CFW-stained septa could be detected in the hyphal cells of ZXB08 (Figure 5B), indicating that overexpression of *paxB* cannot rescue the abolished septation induced by deletion of α-actinin. In contrast, partially restored septum formation was detected when the hyphal cells of ZXB09 (OE-*acnA ΔpaxB*) were stained with CFW (Figure 5, D and E); however, the ZXB09 colonies still had smaller sizes and lacked conidia compared to that of the wild-type strain (Figure 5, C and F), suggesting that overexpression of α-actinin can partially rescue the functions of PaxB in septum formation, but not the functions for the colony growth and conidial production. These data also indicated that the septation and conidiation defects caused by deletion of *paxB* could be partially counteracted by overexpression of α-actinin, but not vice versa, suggesting that α-actinin and PaxB likely have sequential and overlap functions for septation, but may own unique functions for conidiation.

α-Actinin and PaxB belong to an actin cytoskeleton protein network

To determine whether α-actinin, PaxB, and CAR belong to a closely linked protein complex, we searched for

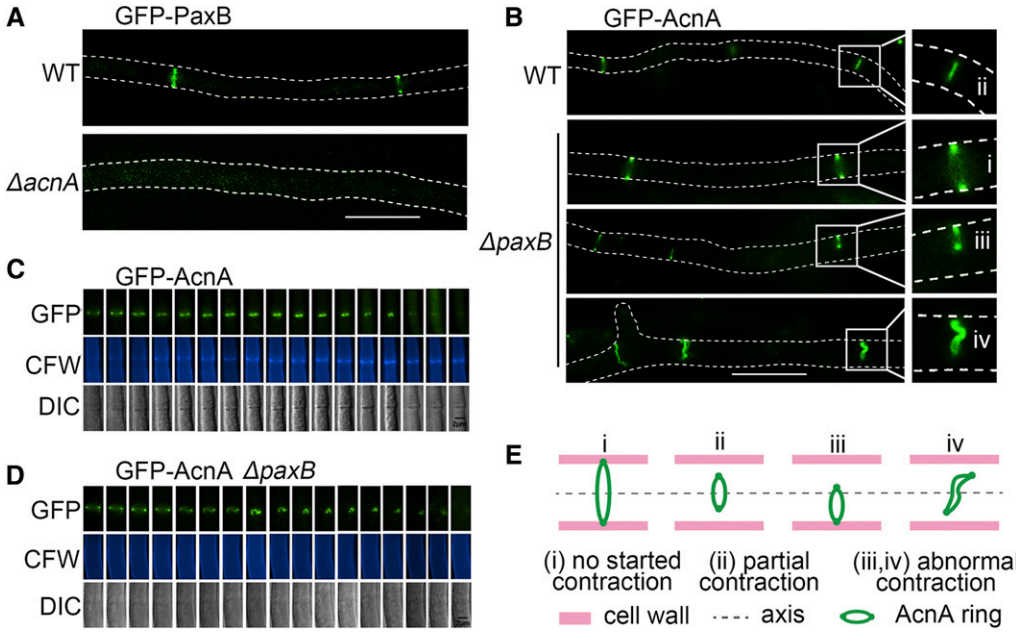

Figure 4 α-Actinin AcnA and PaxB depended on each other with different contents for localization and functions. (A) Localization of GFP-PaxB in the wild-type (AAV98) and *ΔacnA* (ZXB06) strains, and (B) localization of GFP-α-actinin in the wild-type (WJ02) and *ΔpaxB* (ZXB07) strains. All strains were cultured in liquid minimal PGR medium at 37° for 20 hr. Bar, 10 μm. CFW-stained septa, localization of GFP-α-actinin and differential interference contrast (DIC) images of the (C) wild-type (WJ02) and (D) *ΔpaxB* (ZXB07) strains cultured in liquid minimal PGR medium at 37° for 20 hr. Bar, 2 μm. (E) A model for different patterns of the GFP-α-actinin ring.

α-actinin-interacting proteins via a GFP-α-actinin pull-down assay. A strain expressing a GFP-α-actinin fusion protein under the control of a conditional promoter *alc(p)* was used to purify the α-actinin protein complex by exploiting the binding of the GFP tag to GFP-Trap agarose resin. The bound proteins were directly subjected to liquid chromatography–mass spectrometry after proteolytic digestion. A similar approach was used to identify proteins immunoprecipitated by the GFP antibody in strain expressing GFP-tag for eliminating proteins that are pulled down by GFP-tag alone. Consequently, 552 and 390 proteins were identified in the strains expressing GFP-α-actinin and GFP, respectively (Figure 6A and Table S1). After excluding overlapping proteins, 211 specific proteins remained from the collection of proteins identified in the strain expressing GFP-α-actinin. Similarly, the strain expressing PaxB-Flag fusion protein was used to purify the PaxB protein complex by exploiting the binding of the Flag-tag to Flag-Trap agarose resin. To eliminate nonspecific proteins that were pulled down by the Flag-tag, a similar approach was used to identify proteins that were immunoprecipitated by the Flag antibody in a strain expressing only Flag. Liquid chromatography–mass spectrometry identified a total of 529 and 504 proteins in the strains expressing PaxB-Flag and Flag only (Figure 6A and Table S2), respectively. After excluding the overlapping proteins, 107 specific proteins remained from the collection of proteins identified in the strain expressing PaxB-Flag. By comparison, GFP-α-actinin and PaxB-Flag strains shared 34 common proteins (Figure 6B and Table S3). Analysis prediction for these protein functions suggests that 15 and 11 protein homologs have previously been reported and might be involved in the regulation of cytoskeleton and cytokinesis, respectively, as shown in Table S1 (labeled in blue) and Table S2 (labeled in blue), in which they shared nine common cytoskeleton- and cytokinesis-related proteins, as shown in Table S3 (labeled in blue). Moreover, α-actinin as a specific protein was included in the results for the PaxB-Flag strain. To further investigate whether α-actinin directly interacts with PaxB, a co-immunoprecipitation (co-IP) assay was carried out with a GFP-α-actinin and PaxB-Flag double-labeled strain. As co-IP data (Figure S6) showed, no positive band appeared in Western blotting, suggesting that α-actinin and PaxB might not interact directly. According to SMART (http://smart.embl-heidelberg.de/) analysis, α-actinin harbors two CH domains (the actin-binding domain involved in the cross-linking of actin filaments into bundles and to networks) ranging from 12 to 113 amino acids and 126 to 225 amino acids, suggesting that α-actinin might interact with actin directly (Figure 6C). To further investigate network of α-actinin- and actin-interacting proteins, the STRING database (https://string-db.org/) was used to analyze the protein that potentially interacts with the submitted proteins, *i.e.*, α-actinin (AcnA) and actin (ActA), and PaxB. As shown in Figure 6D and Figure S7, α-actinin interacts with actin directly, and four proteins (TpmA, MyoB, FimA, and AN2317) may interact with both α-actinin and actin. Several putative interacting proteins were identified in results of the pull-down assay (labeled in red and green in Figure 6D). Taken together, our results suggest that α-actinin-actin cytoskeleton system and PaxB might belong to a closely linked actin cytoskeleton protein network, which regulates CAR function (Figure 6, D and E).

Discussion

Several lines of evidence have indicated that the proteins of the paxillin family, a class of related and conserved LIM

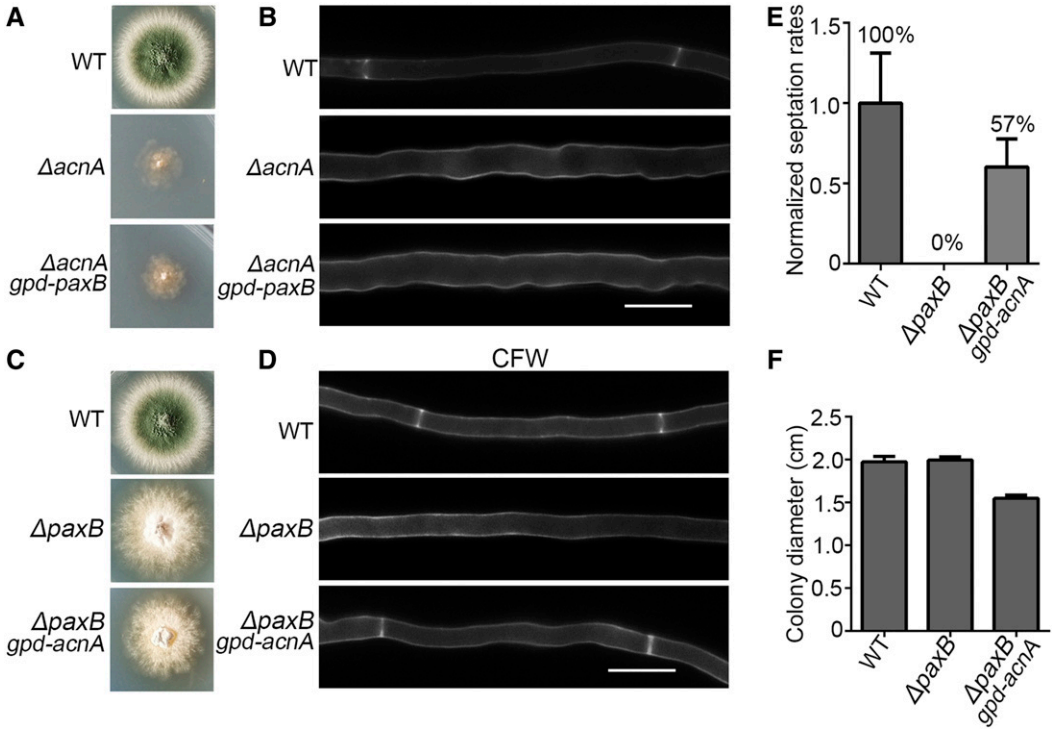

Figure 5 Overexpression of α-actinin partially rescued the defects of the *paxB* mutant in septation. Comparison of the colony morphology (A) in the wild-type, *ΔacnA* (WJ03), and *ΔacnA OE*::*paxB* (ZXB09), and (C) in the wild-type, *ΔpaxB* (AAV127), and *ΔpaxB OE*:: *acnA* (ZXB08) strains. (B and D) Comparison of the septa in hyphal cells stained with CFW for indicated strains cultured in rich YG medium supplemented with 5 mM uridine and 10 mM uracil at 37°. Quantitative data for the septation rates (E) and colony diameters (F) of the respective strains.

domain-containing proteins, play important roles in the transduction of extracellular signals into intracellular responses (Nishiya *et al.* 1999; Brown and Turner 2004; Tanaka *et al.* 2010; Ryan *et al.* 2012). In humans, four isoforms of PXN derived via alternative splicing have been described, all of which provide docking sites for other proteins to facilitate the assembly of multiprotein complexes and act as links from the plasma membrane to the actin cytoskeleton (Salgia *et al.* 1995; Lopez-Colome *et al.* 2017). However, in yeast, only one paxillin protein homolog, Pxl1, has been identified. In the fission yeast *S. pombe*, Pxl1 is localized at cell division sites, where it plays important roles in the formation and contraction of the actomyosin ring and the activation of Rho1 GTPase signaling during cytokinesis. The deletion of Pxl1 leads to abnormal assembly of the actomyosin ring as well as delayed contraction of the CAR (Pinar *et al.* 2008). By comparison, Pxl1 in *S. cerevisiae* localizes to sites of polarized cell growth and acts as a scaffold protein to link cytokinesis signaling with the actin cytoskeleton. Loss of Pxl1 function results in defective polarized cell growth and abnormal mating morphogenesis (Mackin *et al.* 2004). Therefore, based on previously published information on homologous proteins, paxillin proteins are predicted to be required for the assembly and stability of the actin cytoskeleton. Based on the results of a BLAST search, two paxillin proteins, PaxA and PaxB, were identified in *A. nidulans*, and they share 35 and 37% amino acid sequence identity with the paxillin protein Pxl1 in *S. pombe*. Two conserved LIM domains were found in PaxA, while three LIM domains were found in PaxB (Figure 1A). Interestingly, our findings showed that PaxA and PaxB have independent functions. PaxB accumulates robustly at septation sites and is required for septation and cytokinesis via an effect on the CAR formation, while PaxA localizes to the tips of hyphal cells (Figure 1, C and D). However, unexpectedly, there were no detectable defects in the PaxA deletion mutant (Figure 1, B, E, and F). This observation suggests that other alternative candidates might be able to bypass the requirement of PaxA during polar growth in the absence of PaxA.

Similarly, α-actinin is a known scaffold protein that can link the actin cytoskeleton to the plasma membrane or to internal membrane systems (Chan *et al.* 1998). In mammalian cells, α-actinin localizes to the cleavage furrows and participates in the organization of myofibrillar structures during cytokinesis (Jockusch *et al.* 1991). By comparison, a homolog of α-actinin (Ain1) localizes to the actin-containing medial ring during cytokinesis in *S. pombe* (Laporte *et al.* 2012). Cells deleted for Ain1 are unable to form the medial actin ring, resulting in abnormal cytokinesis and septation (Wu *et al.* 2001). Notably, findings in this study combined with those of our previous study showed that the α-actinin homolog in *A. nidulans* is required for cytokinesis/septation and polar hyphal growth for which deletion of *acnA* always shows bipolar hyphal tips. Deletion of α-actinin, an Ain1 homolog, completely abolished septum formation and resulted in a

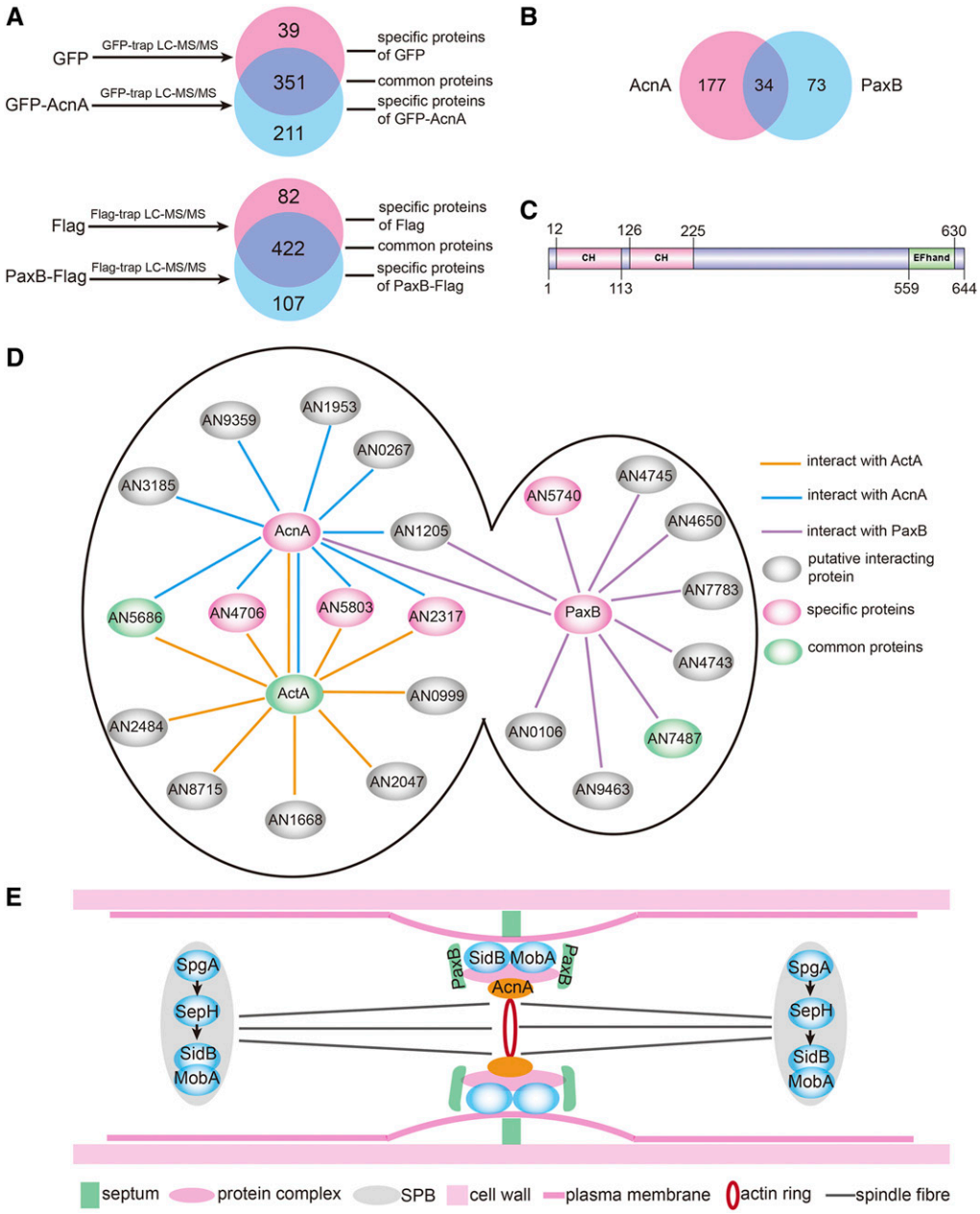

Figure 6 α-Actinin and paxillin B belonged to an actin cytoskeleton protein network. (A) Venn diagram comparison for pull-down protein candidates between GFP-AcnA and GFP alone, and between PaxB-Flag and Flag alone. (B) Venn diagram comparison between GFP-α-actinin and PaxB-Flag pull-down proteins list. (C) Domain analysis of α-actinin via SMART. (D) Analysis of potential α-actinin-, PaxB- and actin-interacting proteins. (E) A schematic model of the regulation of the assembly of the contractile actin ring by α-actinin and PaxB.

fluffy colony phenotype (Wang *et al.* 2009). These defective phenotypes in the α-actinin deletion mutant resemble those caused by the PaxB deletion strain. Thus, we hypothesize that paxillin and actinin in *A. nidulans* may have some sequential and overlapping functions during cytokinesis and septation. In fact, the *paxB* and α-actinin *acnA* deletion strains showed no normal CAR contraction when the final member of the SIN signaling cascade, MobA, was used as CAR marker, suggesting that the function of the CAR was disrupted in the PaxB and α-actinin deletion strains (Figure 2 and Figure 3). However, the data in Figure 5, A and B suggest that PaxB and α-actinin may also have their own independent functions, since overexpression of PaxB was unable to rescue the septation defect in the α-actinin deletion strain, suggesting that PaxB cannot substitute for α-actinin; however, overexpression of α-actinin partly restored septum formation, but not for conidiation in the absence of *paxB*, implying that α-actinin overexpression could bypass the requirement for PaxB to some extent during the process of septum formation. In addition, localization of PaxB to division sites depends on α-actinin, but not vice versa, further demonstrating that α-actinin may play more important roles than PaxB in the function of CAR assembly or during contraction (Figure 4, A and B). On the other hand, PaxB is required for the correct contraction of the α-actinin ring structure (Figure 4), suggesting that both PaxB and α-actinin have important functions in the CAR function during cytokinesis/septation, and that α-actinin may directly interact with actin, while PaxB

probably acts as an accessory to α-actinin to support or stabilize the CAR protein complex, as shown in the model in Figure 6E.

As shown in Figure S2B, colonies for the *alc*(p)*::*gfp-paxB strain displayed no detectable difference compared to that of its parental wild-type strain on the induced medium, suggesting that GFP-PaxB is functional. However, on the repressed minimal medium, the *alc*(p)*::*gfp-paxB strain showed colonies with less conidia compared to the wild-type strain TN02A7, but not as few as observed in the deletion mutant (Figure S2C), implied *paxB* could not be turned-off completely or the truncated version of *paxB* may have partly function. In comparison, in the *alc*(p)*::*gfp-acnA (Wang *et al.* 2009) and *alc::*gfp-mobA (Jiang *et al.* 2018) strains (made previously by a similar strategy as mentioned earlier), phenotypes of colonies on repressed media were equally severe as those observed when the gene was fully deleted, while on the induced medium, they displayed the wild-type-like colony phenotype, suggesting that GFP-AcnA and GFP-MobA labelings were functional and the truncated version of AcnA or MobA in *alc* promoter conditional strains had no functions.

Unexpectedly, our protein interaction studies suggest that α-actinin and PaxB likely do not interact directly since we could not find a positive band by co-IP assay (Figure S6). Another possibility is they interact transiently or display temporal and spatial variation in localization that limits the ability to detect them via co-IP. Compared PaxB-trapping list with that of α-actinin, they shared 34 common specific proteins, many of which may be involved in the function of the actin cytoskeleton system (Table S3), which suggests that α-actinin and PaxB may belong to a closely linked actin cytoskeleton protein network.

Taken together, our findings suggest that the scaffold proteins PaxB and α-actinin and the SIN signal work in harmony together, and each of them is required for cytokinesis/septation and conidiation, probably via influencing CAR formation and contraction.

Acknowledgments

This work was financially supported by the National Key Research and Development Program of China (grant 2019YFA0904900), the National Natural Science Foundation of China (grants NSFC31861133014 and 31770086), the Program for Jiangsu Excellent Scientific and Technological Innovation team (grant 17CXTD00014), the Priority Academic Program Development of Jiangsu Higher Education Institutions. The funders had no role in study.

Literature Cited

Akamatsu, M., J. Berro, K. M. Pu, I. R. Tebbs, and T. D. Pollard, 2014 Cytokinetic nodes in fission yeast arise from two distinct types of nodes that merge during interphase. J. Cell Biol. 204: 977–988. https://doi.org/10.1083/jcb.201307174

Bergs, A., Y. Ishitsuka, M. Evangelinos, G. U. Nienhaus, and N. Takeshita, 2016 Dynamics of actin cables in polarized growth of the filamentous fungus *Aspergillus nidulans*. Front. Microbiol. 7: 682. https://doi.org/10.3389/fmicb.2016.00682

Bi, E., and H. O. Park, 2012 Cell polarization and cytokinesis in budding yeast. Genetics 191: 347–387. https://doi.org/10.1534/genetics.111.132886

Brown, M. C., and C. E. Turner, 2004 Paxillin: adapting to change. Physiol. Rev. 84: 1315–1339. https://doi.org/10.1152/physrev.00002.2004

Bruno, K. S., J. L. Morrell, J. E. Hamer, and C. J. Staiger, 2001 SEPH, a Cdc7p orthologue from *Aspergillus nidulans*, functions upstream of actin ring formation during cytokinesis. Mol. Microbiol. 42: 3–12. https://doi.org/10.1046/j.1365-2958.2001.02605.x

Chan, Y., H. Q. Tong, A. H. Beggs, and L. M. Kunkel, 1998 Human skeletal muscle-specific alpha-actinin-2 and -3 isoforms form homodimers and heterodimers in vitro and in vivo. Biochem. Biophys. Res. Commun. 248: 134–139. https://doi.org/10.1006/bbrc.1998.8920

Cheffings, T. H., N. J. Burroughs, and M. K. Balasubramanian, 2016 Actomyosin ring formation and tension generation in eukaryotic cytokinesis. Curr. Biol. 26: R719–R737. https://doi.org/10.1016/j.cub.2016.06.071

Corbett, M., Y. Xiong, J. R. Boyne, D. J. Wright, E. Munro *et al.*, 2006 IQGAP and mitotic exit network (MEN) proteins are required for cytokinesis and re-polarization of the actin cytoskeleton in the budding yeast, *Saccharomyces cerevisiae*. Eur. J. Cell Biol. 85: 1201–1215. https://doi.org/10.1016/j.ejcb.2006.08.001

Cortés, J. C. G., M. Konomi, I. M. Martins, J. Munoz, M. B. Moreno *et al.*, 2007 The (1,3)beta-D-glucan synthase subunit Bgs1p is responsible for the fission yeast primary septum formation. Mol. Microbiol. 65: 201–217. https://doi.org/10.1111/j.1365-2958.2007.05784.x

Cortés, J. C. G., N. Pujol, M. Sato, M. Pinar, M. Ramos *et al.*, 2015 Cooperation between paxillin-like protein Pxl1 and glucan synthase Bgs1 is essential for actomyosin ring stability and septum formation in fission yeast. PLoS Genet. 11: e1005358. https://doi.org/10.1371/journal.pgen.1005358

Courtemanche, N., 2018 Mechanisms of formin-mediated actin assembly and dynamics. Biophys. Rev. 10: 1553–1569. https://doi.org/10.1007/s12551-018-0468-6

D'Avino, P. P., 2009 How to scaffold the contractile ring for a safe cytokinesis - lessons from Anillin-related proteins. J. Cell Sci. 122: 1071–1079. https://doi.org/10.1242/jcs.034785

D'Avino, P. P., M. G. Giansanti, and M. Petronczki, 2015 Cytokinesis in animal cells. Cold Spring Harb. Perspect. Biol. 7: a015834. https://doi.org/10.1101/cshperspect.a015834

Evangelista, M., D. Pruyne, D. C. Amberg, C. Boone, and A. Bretscher, 2002 Formins direct Arp2/3-independent actin filament assembly to polarize cell growth in yeast. Nat. Cell Biol. 4: 32–41. https://doi.org/10.1038/ncb718

Ge, W. Z., and M. K. Balasubramanian, 2008 Pxl1p, a paxillin-related protein, stabilizes the actomyosin ring during cytokinesis in fission yeast. Mol. Biol. Cell 19: 1680–1692. https://doi.org/10.1091/mbc.e07-07-0715

Green, R. A., E. Paluch, and K. Oegema, 2012 Cytokinesis in animal cells. Annu. Rev. Cell Dev. Biol. 28: 29–58. https://doi.org/10.1146/annurev-cellbio-101011-155718

Gupta, S. K., K. K. Maggon, and T. A. Venkitasubramanian, 1976 Effect of zinc on adenine nucleotide pools in relation to aflatoxin biosynthesis in *Aspergillus parasiticus*. Appl. Environ. Microbiol. 32: 753–756. https://doi.org/10.1128/AEM.32.6.753-756.1976

Harris, S. D., 2001 Septum formation in *Aspergillus nidulans*. Curr. Opin. Microbiol. 4: 736–739. https://doi.org/10.1016/S1369-5274(01)00276-4

Jiang, P., W. F. Wei, G. W. Zhong, X. G. Zhou, W. R. Qiao *et al.*, 2017 The function of the three phosphoribosyl pyrophosphate synthetase (Prs) genes in hyphal growth and conidiation in *Aspergillus nidulans*. Microbiology 163: 218–232. https://doi.org/10.1099/mic.0.000427

Jiang, P., S. Zheng, and L. Lu, 2018 Mitotic-Spindle organizing protein MztA mediates septation signaling by suppressing the regulatory subunit of protein phosphatase 2A-ParA in *Aspergillus nidulans*. Front. Microbiol. 9: 988. https://doi.org/10.3389/fmicb.2018.00988

Jockusch, B. M., B. Zurek, R. Zahn, A. Westmeyer, and A. Fuchtbauer, 1991 Antibodies against vertebrate microfilament proteins in the analysis of cellular motility and adhesion. J. Cell Sci. Suppl. 14: 41–47. https://doi.org/10.1242/jcs.1991.Supplement_14.9

Kim, J. M., L. Lu, R. Shao, J. Chin, and B. Liu, 2006 Isolation of mutations that bypass the requirement of the septation initiation network for septum formation and conidiation in *Aspergillus nidulans*. Genetics 173: 685–696. https://doi.org/10.1534/genetics.105.054304

Laporte, D., R. Zhao, and J. Q. Wu, 2010 Mechanisms of contractile-ring assembly in fission yeast and beyond. Semin. Cell Dev. Biol. 21: 892–898. https://doi.org/10.1016/j.semcdb.2010.08.004

Laporte, D., N. Ojkic, D. Vavylonis, and J. Q. Wu, 2012 alpha-Actinin and fimbrin cooperate with myosin II to organize actomyosin bundles during contractile-ring assembly. Mol. Biol. Cell 23: 3094–3110. https://doi.org/10.1091/mbc.e12-02-0123

Li, Y., J. R. Christensen, K. E. Homa, G. M. Hocky, A. Fok *et al.*, 2016 The F-actin bundler alpha-actinin Ain1 is tailored for ring assembly and constriction during cytokinesis in fission yeast. Mol. Biol. Cell 27: 1821–1833. https://doi.org/10.1091/mbc.e16-01-0010

Liu, B., X. Xiang, and Y. R. Lee, 2003 The requirement of the LC8 dynein light chain for nuclear migration and septum positioning is temperature dependent in *Aspergillus nidulans*. Mol. Microbiol. 47: 291–301. https://doi.org/10.1046/j.1365-2958.2003.03285.x

Lopez-Colome, A. M., I. Lee-Rivera, R. Benavides-Hidalgo, and E. Lopez, 2017 Paxillin: a crossroad in pathological cell migration. J. Hematol. Oncol. 10: 50. https://doi.org/10.1186/s13045-017-0418-y

Mackin, N. A., T. J. Sousou, and S. E. Erdman, 2004 The PXL1 gene of *Saccharomyces cerevisiae* encodes a paxillin-like protein functioning in polarized cell growth. Mol. Biol. Cell 15: 1904–1917. https://doi.org/10.1091/mbc.e04-01-0004

McGuire, S. L., D. L. Roe, B. W. Carter, R. L. Carter, S. P. Grace *et al.*, 2000 Extragenic suppressors of the nimX2(cdc2) mutation of *Aspergillus nidulans* affect nuclear division, septation and conidiation. Genetics 156: 1573–1584.

Mela, A., and M. Momany, 2019 Septin mutations and phenotypes in *S. cerevisiae*. Cytoskeleton (Hoboken) 76: 33–44. https://doi.org/10.1002/cm.21492

Mulvihill, D. P., C. Barretto, and J. S. Hyams, 2001 Localization of fission yeast type II myosin, Myo2, to the cytokinetic actin ring is regulated by phosphorylation of a C-terminal coiled-coil domain and requires a functional septation initiation network. Mol. Biol. Cell 12: 4044–4053. https://doi.org/10.1091/mbc.12.12.4044

Muñoz, J., J. C. G. Cortes, M. Sipiczki, M. Ramos, J. A. Clemente-Ramos *et al.*, 2013 Extracellular cell wall β(1,3)glucan is required to couple septation to actomyosin ring contraction. J. Cell Biol. 203: 265–282. https://doi.org/10.1083/jcb.201304132

Nishiya, N., Y. Iwabuchi, M. Shibanuma, J. F. Cote, M. L. Tremblay *et al.*, 1999 Hic-5, a paxillin homologue, binds to the protein-tyrosine phosphatase PEST (PTP-PEST) through its LIM 3 domain. J. Biol. Chem. 274: 9847–9853. https://doi.org/10.1074/jbc.274.14.9847

Osmani, S. A., R. T. Pu, and N. R. Morris, 1988 Mitotic induction and maintenance by overexpression of a G2-specific gene that encodes a potential protein kinase. Cell 53: 237–244. https://doi.org/10.1016/0092-8674(88)90385-6

Pearson, C. L., K. Xu, K. E. Sharpless, and S. D. Harris, 2004 MesA, a novel fungal protein required for the stabilization of polarity axes in *Aspergillus nidulans*. Mol. Biol. Cell 15: 3658–3672. https://doi.org/10.1091/mbc.e03-11-0803

Pinar, M., P. M. Coll, S. A. Rincon, and P. Perez, 2008 *Schizosaccharomyces pombe* Pxl1 is a paxillin homologue that modulates Rho1 activity and participates in cytokinesis. Mol. Biol. Cell 19: 1727–1738. https://doi.org/10.1091/mbc.e07-07-0718

Pollard, T. D., and J. Q. Wu, 2010 Understanding cytokinesis: lessons from fission yeast. Nat. Rev. Mol. Cell Biol. 11: 149–155. https://doi.org/10.1038/nrm2834

Ryan, P. E., S. C. Kales, R. Yadavalli, M. M. Nau, H. Zhang *et al.*, 2012 Cbl-c ubiquitin ligase activity is increased via the interaction of its RING finger domain with a LIM domain of the paxillin homolog, Hic 5. PLoS One 7: e49428. https://doi.org/10.1371/journal.pone.0049428

Salgia, R., J. L. Li, S. H. Lo, B. Brunkhorst, G. S. Kansas *et al.*, 1995 Molecular cloning of human paxillin, a focal adhesion protein phosphorylated by P210BCR/ABL. J. Biol. Chem. 270: 5039–5047. https://doi.org/10.1074/jbc.270.10.5039

Shao, H., J. H. C. Wang, M. R. Pollak, and A. Wells, 2010 α-Actinin-4 is essential for maintaining the spreading, motility and contractility of fibroblasts. PLoS One 5: e13921. https://doi.org/10.1371/journal.pone.0013921

Tanaka, T., K. Moriwaki, S. Murata, and M. Miyasaka, 2010 LIM domain-containing adaptor, leupaxin, localizes in focal adhesion and suppresses the integrin-induced tyrosine phosphorylation of paxillin. Cancer Sci. 101: 363–368. https://doi.org/10.1111/j.1349-7006.2009.01398.x

Todd, R. B., M. A. Davis, and M. J. Hynes, 2007 Genetic manipulation of *Aspergillus nidulans*: heterokaryons and diploids for dominance, complementation and haploidization analyses. Nat. Protoc. 2: 822–830. https://doi.org/10.1038/nprot.2007.113

Turner, C. E., N. Kramarcy, R. Sealock, and K. Burridge, 1991 Localization of paxillin, a focal adhesion protein, to smooth muscle dense plaques, and the myotendinous and neuromuscular junctions of skeletal muscle. Exp. Cell Res. 192: 651–655. https://doi.org/10.1016/0014-4827(91)90090-H

Vargas-Muñiz, J. M., H. Renshaw, A. D. Richards, F. Lamoth, E. J. Soderblom *et al.*, 2015 The *Aspergillus fumigatus* septins play pleiotropic roles in septation, conidiation, and cell wall stress, but are dispensable for virulence. Fungal Genet. Biol. 81: 41–51. https://doi.org/10.1016/j.fgb.2015.05.014

von Dassow, G., 2009 Concurrent cues for cytokinetic furrow induction in animal cells. Trends Cell Biol. 19: 165–173. https://doi.org/10.1016/j.tcb.2009.01.008

Wang, J., H. Hu, S. Wang, J. Shi, S. Chen *et al.*, 2009 The important role of actinin-like protein (AcnA) in cytokinesis and apical dominance of hyphal cells in *Aspergillus nidulans*. Microbiology 155: 2714–2725. https://doi.org/10.1099/mic.0.029215-0

Watanabe, S., Y. Ando, S. Yasuda, H. Hosoya, N. Watanabe *et al.*, 2008 mDia2 induces the actin scaffold for the contractile ring and stabilizes its position during cytokinesis in NIH 3T3 cells. Mol. Biol. Cell 19: 2328–2338. https://doi.org/10.1091/mbc.e07-10-1086

Wu, J. Q., J. Bahler, and J. R. Pringle, 2001 Roles of a fimbrin and an alpha-actinin-like protein in fission yeast cell polarization

and cytokinesis. Mol. Biol. Cell 12: 1061–1077. https://doi.org/10.1091/mbc.12.4.1061

Yumura, S., and T. Kitanishi-Yumura, 1990 Fluorescence-mediated visualization of actin and myosin filaments in the contractile membrane-cytoskeleton complex of *Dictyostelium discoideum*. Cell Struct. Funct. 15: 355–364. https://doi.org/10.1247/csf.15.355

Zheng, S., F. Dong, F. Rasul, X. Yao, Q. W. Jin *et al.*, 2018 Septins regulate the equatorial dynamics of the separation initiation network kinase Sid2p and glucan synthases to ensure proper cytokinesis. FEBS J. 285: 2468–2480. https://doi.org/10.1111/febs.14487

Communicating editor: N. Louise Glass